Materials Science and Technology, Volume 25, Number 11, November 2009, Pages 1307-1311

Nanocoatings on micro- or nano-particles

Z. Libor[1], Q. Zhang[1]*, C. Israel[2], N. D. Mathur[2]

[1]Department of Advanced Materials, Cranfield University, Bedfordshire, MK43 0AL, UK
[2]Department of Materials Science, University of Cambridge, Cambridge CB2 3QZ, UK

*Corresponding author e-mail: q.zhang@cranfield.ac.uk)

Abstract

In recent years, coating processes with nanoparticles have been investigated for the development of nanostructured materials. In this work we report the core-shell structures of micro-composites of SiO_2/Ni, SiO_2/Fe_3O_4, and nano-composites of $BaTiO_3/Fe_3O_4$ and PZT/Fe_3O_4. These composites were prepared by an aqueous chemical synthesis method and characterised by scanning electron microscopy (SEM), X-ray diffraction (XRD), Energy Dispersive X-Ray (EDX) analysis and Vibrating Sample Magnetometry (VSM) before and after incorporation into the core-shell structure. The composite core-shell structures were formed by the control of the surface charges of particles in aqueous solutions. A specific composite (SiO_2/Ni, SiO_2/Fe_3O_4 and $BaTiO_3/Fe_3O_4$ and PZT/Fe_3O_4 nano-composites) can be produced by controlling the pH and the molar ratio of components. These magnetic composites can be potentially applied in wide range of fields such as micro-reactors, delivery vehicle systems, drug delivery systems and multiferroics.

Introduction

In recent years, core-shell structural composites have also attracted interest due to their coupling properties. Hybrid materials with core-shell structure are usually composed of microspheric cores shelled with nanoparticles. The coating of nanoparticles on the core particles can be formed either by direct surface reactions or by controlled precipitation of the nanoparticles on the surfaces of the suspended spherical cores [1,2]. Such materials may exhibit many unique electrical, magnetic, optical or mechanical properties and therefore have attracted extensive scientific and technological interests [2,3,4]. For example, some biomedical applications, such as, tagging, imaging, sensing and separation [5,6], require core-shell magnetic nanoparticles. The most promising applications for core-shell magnetic nanoparticles relate to the diagnosis and treatment of cancer [7,8].

The magnetoelectric effect between two materials, such as a ferromagnet and a ferroelectric, relies upon indirect coupling, via strain [9]. Strain coupling requires intimate contact between a magnetostrictive (or piezomagnetic) material and a piezoelectric (or electrostrictive) material. This can be achieved in composite and core-shell structures where the interfacial area is large.
Applications of small particles with micro- or nano-core-shell structure need to meet two basic requirements: a designable coating layer on the core particles and economical synthesis. The core-shell particles with inorganic coatings offer interesting prospects in fabricating a broad range of materials with different properties. From economical and environmental points of view, an aqueous method is preferable [10]. The processing of monodispersed nanopowders has been successfully adopted; however, the methods to obtain nanocoatings are not well developed up to now. In the meantime, a wide variety of methods have been explored and developed for the synthesis of well defined coated powders, such as, heterogeneous precipitation [4], sol-gel process [11], hydrothermal synthesis [12], homogeneous precipitation [13], electrochemical method [3], inverse microemulsion [14], emulsion evaporation [15], and spray drying [16].

In this study, we fabricated the various micro- or nano-particles using different chemical synthesis methods. The core-shell nanocomposites were fabricated using the immobilization of prepared magnetic Ni or Fe_3O_4 nanoparticles on the surface of SiO_2 or ferroelectric $BaTiO_3$ or $Pb(Zr,Ti)O_3$ particles by adjusting pH values in order to control their zeta potential. Moreover, the structural as well as magnetic differences between the composites with different sized cores have been compared.

Experimental

Preparation of nanoparticles. Magnetic Fe_3O_4 nanoparticles were synthesized by a chemical solution method described in [17]. The hollow silica particles were synthesized by a combination of sol-gel process and water-in-oil (W/O) emulsion based on the work described in [18]. The final powder was calcined at 700 ^oC for 8 hrs in a furnace. Monodisperse nickel nanopowders were synthesized by wet-chemical method [19]. BT and PZT nanoparticles were synthesized by hydrothermal synthesis described by Clark [5] and by Deng [6].

Preparation of Ni- and Fe_3O_4 - coated SiO_2, BT, and PZT particles. For the synthesis of core-shell structures the core particles, for example SiO_2, BT or PZT were suspended in deionised water in a volumetric flask with a concentration of 0.1g/L. The suspension was then placed in an ultrasonic bath for 30 min. At this point, the pH of the suspension was adjusted by adding HCl or KOH to the value given by the measurement of Zeta potential. Similarly, in another volumetric flask, Ni or Fe_3O_4 shell particles were suspended in deionised water and the particle concentration was dependent on the coated thickness. The suspension was also placed in an ultrasonic bath for 30 min and the pH of the suspension was adjusted as for the core solutions. Based on the measurements of Zeta potential of particle colloids in water, core and shell particles would produce opposite surface charges at the certain pH regions. The core and shell particle colloids with such pH values were then mixed and placed to the orbital shaker for 30 min. The electrostatic force on the surfaces of the core and shell particles would make the attraction of different charged particles to each other and thus form a core-shell structure. The core-shell particles were then dried in the oven at 40 ºC overnight.

Structural and magnetic characterization. Transmission electron microscopy (TEM) was performed on a Philips CM 20 operating at 200 kV, and scanning electron microscopy (S-FEG SEM) was performed on a Philips XL30. X-ray diffraction (XRD) patterns were obtained using a Siemens D5005 diffractometer with CuKα radiation and a Goebel mirror. The crystallite size is determined from the X-ray line broadening using Scherrer formula given by $D = 0.9\ \lambda / \beta \cos \theta$, where D is the average crystallite size, λ is the X-ray wavelength used (1.5406 Å), β is the angular line width of half maximum intensity and θ is the Bragg's angle in degree. The pH values of particles in water were measured using a Jenway 3540 pH meter. Electrophoresis measurements were performed using a Malvern Zetasizer 3000. The magnetic properties of the products were characterized using a Princeton Measurements Corporation vibrating sample magnetometer (VSM)**.**

Results and discussion

Fig. 1 shows the SEM images of (a) Ni and the TEM image of (b) Fe_3O_4. The average size of SiO_2, BT, PZT, Ni and Fe_3O_4 particles is about 15 μm, 130 nm, 1 μm, 90 ~100 nm and 10 nm, respectively. SiO_2, BT and Ni particles are spherical while PZT particles are more or less cubic. Except for SiO_2, all the particles showed a narrow particle distribution. Due to the large surface to volume ratio and strong magnetic attraction forces, the Ni and Fe_3O_4 nanoparticles tend to agglomerate in order to minimize the total surface energy of the system.

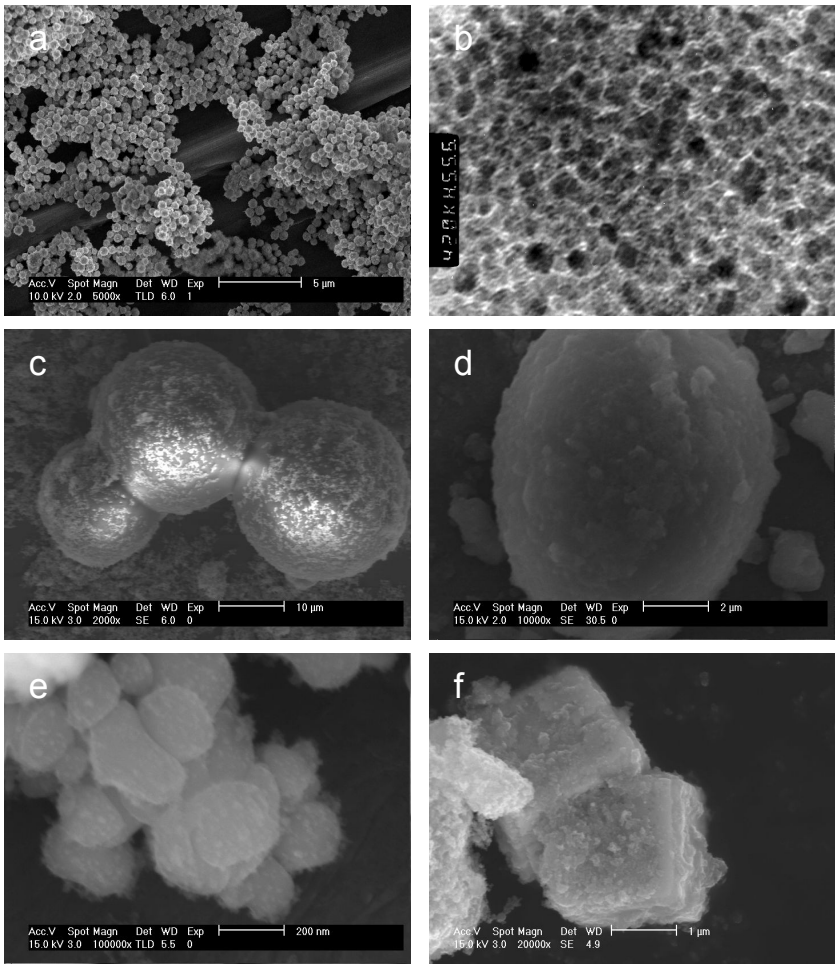

Figure 1: SEM and TEM images of particles and core-shell particles. a: Ni ; b: Fe_3O_4 (TEM); c: SiO_2/Ni; d: SiO_2/Fe_3O_4; e:BT/Fe_3O_4; f: PZT/Fe_3O_4.

Fig. 2 shows the zeta potential values of the SiO_2, BT, PZT, Fe_3O_4 and Ni particles in water as a function of pH. Zeta potential measurement gives the information about the overall surface charge of the particles and how this is affected by the changes in the environment (e.g. pH). The measured colloid suspensions were prepared without adding any surfactant. The results of the electrophoresis measurements revealed that the zeta potentials of core (SiO_2, BT and PZT) and shell (Ni and Fe_3O_4) particles have opposite signs in some pH regions, for example, at $4.3 < pH < 9.0$, the zeta potential for SiO_2 particles was between 0 and - 40 mV while the zeta potential of Fe_3O_4 particles was between +30 and 0 mV. This allowed for the easy attachment of the Fe_3O_4 particles on the surface of SiO_2 particles at this pH region, similarly, of the Ni particles on the surface of SiO_2 particles at $4.3 < pH < 10.7$, of the Fe_3O_4 particles on the surface of BT and PZT particles at $4.2 < pH < 9.0$ and $5.1 < pH < 9.0$, respectively.

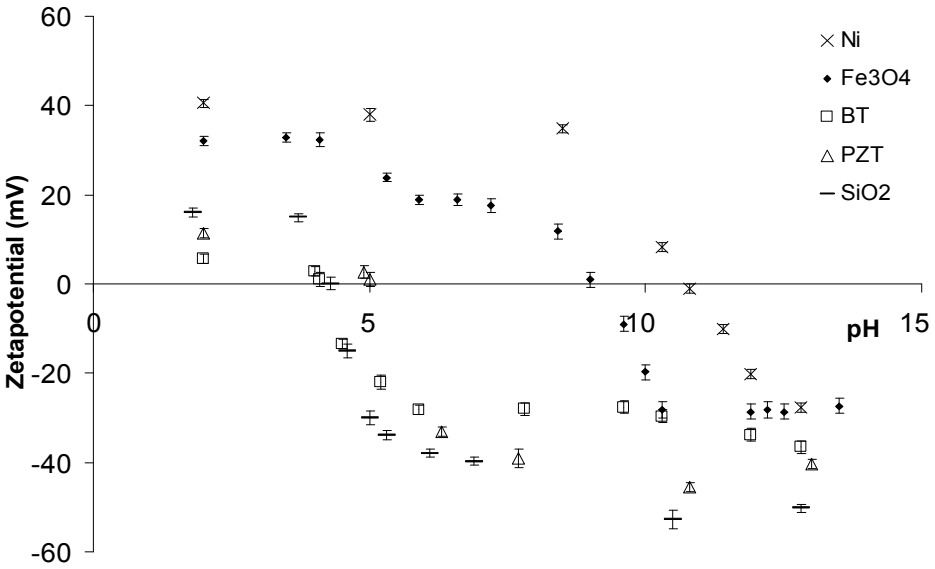

Figure 2: Zeta potentials of SiO_2, $BaTiO_3$, PZT, Fe_3O_4 and Ni particles in water as function of pH. Adjustment of the pH was carried out by adding standard HCl and KOH solutions.

SEM was also employed to examine the morphology of the coated particles (Fig 1, c-f). In comparison with the neat particles (Fig1, a-b), the coated particles have a rough surface. The ferrite coating is confirmed from the change in size, shape and the presence of Fe element in the particle determined from EDX (data not shown). The SiO_2 particles remain spherical after they were coated with Ni (Fig 1, c) or Fe_3O_4 (Fig 1, d). The PZT crystals with cubic shape have a smooth edge after they were coated with Fe_3O_4 (Fig 1, f). The thickness of the shell can be controlled through the mediation of the ratio of core and shell particles and the reaction time. It is worth to note that the higher the shell particle concentration is, the rougher the coated surface is. This is understandable because the higher concentration of shell particles leads to multi-layer coating. Shell morphology is strongly dependent on the parameters, such as, pH values, suspension concentration and the core-shell particle ratio.

XRD patterns for core-shell particles (such as SiO_2/Ni, SiO_2/Fe_3O_4, $BaTiO_3/Fe_3O_4$ and PZT/Fe_3O_4) have been carried out (data not shown). For the purpose of comparison, the XRD patterns of the core and the shell particles were also measured (data not shown). In the case of Ni particles and Ni coated SiO_2, three characteristic peaks for nickel (2θ = 44.5º, 51.8º, and 76.4º), corresponding to Miller indices (111), (200), and (222), were observed. This revealed that the resultant particles were pure face-centred cubic (fcc) nickel at both samples (JCPDS, No. 04-0850). The XRD patterns reveal that only nickel is detected. Although it is known that nickel is easily oxidized to oxides, some possible oxides such as NiO, Ni_2O_3 are not observed in the XRD profiles. Because the core-shell samples have been exposed to the air and water for a long time during the synthesis, the absence of nickel oxides also indicates that the current synthetic method for Ni coated core-shell structure is feasible in achieving metallic Ni coated core-shell structure. The calculated size values for both pure Ni and coated Ni by Scherrer formula at 2θ of 44.5º are general approximates to that of SEM observation (Fig. 1).

The Fe_3O_4 coated particles were measured in the VSM at 300 K. Fig. 3 shows the magnetization versus field plots of the Fe_3O_4-coated particles. The magnetic curves of three samples exhibit ferromagnetic behaviour (hysteresis can be seen in the inset of Fig. 3). All of the samples possess a lower saturation magnetization M_s (Table 1) than bulk Fe_3O_4 (92 emu/g) [20] due to the presence of the SiO_2, BT or PZT. After normalizing the M_s values of core-shell particles to emu per gram of bare 10 nm Fe_3O_4 nanoparticles (53.8 emu/g [21,22]), the weight percentage of shell can be crudely estimated (Table 1). Under the same conditions, the content of Fe_3O_4 coated on the different surfaces is varied and this might be related to the relative size of core and shell particles, their attractive force, and particle geography. The magnetic properties of Ni coated SiO_2 particles were also measured at 300 K (data not shown) and M_s=7.8 emu/g is 14% of the bulk value (55 emu/g) [23] due to the presence of the SiO_2 and e.g. surface oxidation.

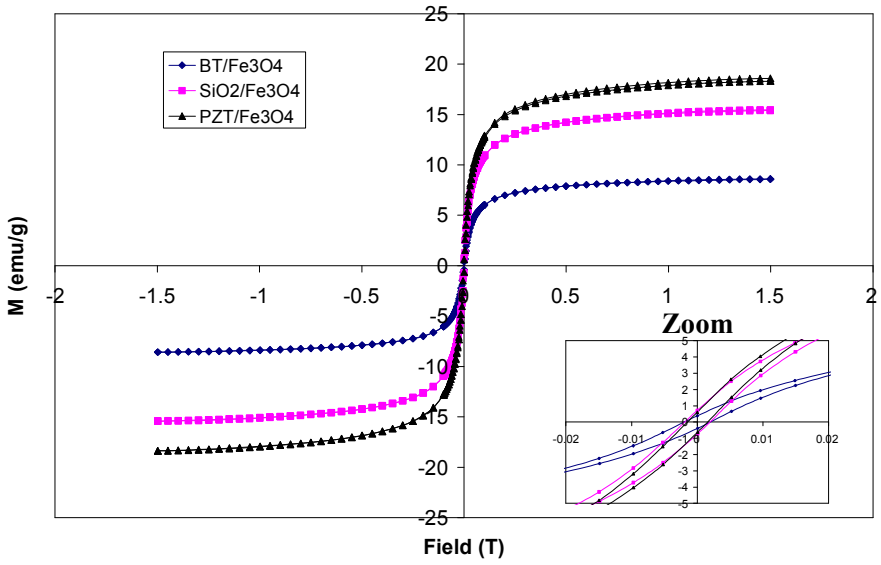

Figure 3: Magnetization as a function of applied magnetic field for Fe_3O_4 coated particles at room temperature. Inset: hysteresis is seen at low-fields.

Table1: Magnetization data for various samples measured at room temperature.

Sample	M_s (emu/g)	Content $_{shell}$ (%)
BT/Fe_3O_4	8.6	16
SiO_2/Fe_3O_4	15.4	29
PZT/Fe_3O_4	18.3	34
SiO_2/Ni	7.8	14

Conclusions

Various micro-, nano-particles have been synthesised using chemical methods. Using a simple method, e.g. controlling the solution's pH value and thus the surface charges of core and shell particles, magnetic nanoparticles of Fe_3O_4 and Ni were used to successfully coat the SiO_2, BT and PZT particles in an aqueous solution. The resultant core-shell nanostructures were examined using XRD, SEM, TEM and EDX. Shell thickness can be controlled through various parameters. The saturation magnetizations of the Fe_3O_4 and Ni-coated particles were reduced by the presence of the non-magnetic core, which permits an estimate of the weight fractions.

References

1. Philipse, A.P., Van Bruggen, M.P.B. & Pathmamanoharan, C., Langmuir, 10 145 (1994)
2. Caruso, F, Chem. Eur. J., 6, 413 (2000)
3. Kim, S.H., Kim, M.J. & Choa, Y.H., Materials Science and Engineering A, 449-451, 386 (2007)
4. Villegas, M., Sirerra, T., Caballero, A.C. & Fernandez, F.J., Ceramics International, 33, 875 (2007)
5. Clark, I.J. & Takeuchi, T., J. Mater. Chem., 9, 83 (1999)
6. Deng, Y., Liu, L., Cheng, Y. & Nan, C.W., Materials Letter, 57, 1675 (2003)
7. Pankhrust, Q.A., Connolly, J. Jones, S.K. & Dobson, J., J.Phys. D; Appl.Phys., 36, 167 (2003)
8. Arruebo, M., Pacheco, R.F., Ibarra, R. & Santamaria, J., Nanotoday, 12(3), 22 (2007)
9. Eerenstein, W., Mathur, N.D. & Scott, J.F., Nature, 442, 759 (2006)
10. Wang, K., Tan, W. & He, X., IEEE, Engineering in Medicine and Biology, 27 Conference, Shanghai (2007)
11. Sugimoto,T., Zhou, X. & Muramatsu, A., J. Colloid. Interface Sci., 259(1), 43 (2003)
12. Yang, J., Mei, S. & M. Ferreira, J.M., J. Am. Ceram. Soc., 84(8), 1696 (2001)
13. Lee, K.R., Kim, S.J., Song, J.S., Lee, J.H., Chung, Y. J.& Park, S., J.Am. Ceram. Soc., 85(2), 341 (2002)
14. Wang, G. & Li, G., Eur. Phys. J. D, 24, 355 (2003)
14. Landfester, K., Adv. Mater., 13(10), 765 (2001)
16. Kim, J., Wilhelm, O. & Pratsinis,S.E., Adv. Eng. Mater., 4(7), 494 (2002)
17. Shan, G.B., Xing, J.M., Zhang, H.Y. & Liu, H.Z., Appl. and Environm. Microbiology, 71(8), 4497 (2005)
18. Li, W., Sha, X., Dong, W. & Wang, Z., Chem.Commun., 2434 (2002)
19. Choi, J.Y., Lee, K.Y., Kim, B.K. & Kim, J.M., J.Am.Ceram.Soc., 88[11], 3020 (2005)
20. Zhang, M., Zhang, Q., Itoh, T. & Abe, M., IEEE Trans. Magn., 30, 4692 (1994)
21. Huang, C.K., Hou, C.H., Chen, C.C., Tsai, Y.L., Chang, L.M., Wei, H.S., Hsieh, K.S. & Chan, C.H., Nanotechnology, 19, 055701 (2008)
22. Lee, J., Isobe, T. & Senna, M., J. Colloid Interface Sci., 177, 490 (1996)
23. Cullity, B.D., Introduction to Magnetic Materials, Addison Wesley, New York, p. 129 (1972)